Proceedings of the World Congress on Engineering 2014 Vol I,
WCE 2014, July 2 - 4, 2014, London, U.K.

The Study of Half-Bridge Currents Converter

Guo-Shing Huang, *Senior Member, IEEE*, Shing-Lih Wu and Zi-Sheng Lin

***Abstract*—In this paper, the main purpose is to investigate the half-bridge converter and inductors which is winded by both sides of coils. Therefore, it also focuses on different kinds of inductors. To discuss the function of signal isolation and anti-electromagnetic interference under different kinds of inductors, the input and output currents have the performance of continuous and discontinuous conductance. Finally, the study aims at different frequencies to compare half-bridge circuits with commercial inductors; in addition, improve the noise jamming waveform.**

***Index Terms*—Half-Bridge, Inductor, PWM**

I. Introduction

In recent years, global environmental pollution problems become serious day by day, and it reflects human environment. In order to avoid ecological damages becoming more serious**,** green energy technology plays an important role and also for future main stream. Nowadays, there are many kinds of green energy technology. Take electric vehicles for example, to electrify batteries is particularly significant. To lengthen the life-span of batteries and prevent the battery temperatures from being over high, it studies aiming at charging converters [1-3]. For step-up and buck circuits of converters, there are both including the characteristic of discontinuous input and output currents. However, it produces the flaws of electromagnetic interference (EMI) and high output noise. And the drawback of full-bridge transformer switching mode power supply is higher power outage. Hence, full-bridge transformer switching mode power supply should not be used under low voltage to make low working efficiency. In our study, combine circuits with half-bridge circuits to improve above-mentioned shortcomings. Employ the functions of inductors which are stored energy, varying voltage and separation, and focus on improving inductor output waveform.

In terms of signal processing, half-bridge circuits in our study are better than full-bridge circuits. Because full-bridge circuits operate with four transistor switches for input signal, it should include the current switching with two transistor switches being simultaneous conduction and two transistor switches being simultaneous cut. In that way, signal processing is more difficult and complex. However, for half-bridge circuits, it operates the current switching with two transistor switches for input signal; its current switching works under one transistor switch conducting and one transistor switch cutting. In this way, signal processing is more easy and simple. It promotes endured output load with dual transistors switch; therefore, power value of load output in study can bear about 1kW [5]. In study, it tests different frequencies comparing commercial inductors with developed inductors in order to select the best inductor for experiment. We inform by experimental data that, in this study, developed inductors can improve noise problems effectively and contain advantages of higher power output power, high working efficiency, small circuits, tractable signals, low costs and smaller gains and dynamic ranges of error amplifiers.

The following sequentially is the second part of overall system architecture [6-8], the third part of system design [9-11], the fourth part of experimental test results, and finally the fifth part of conclusion of features and advantages on software and hardware.

Manuscript received March 13, 2014; revised March 30, 2014. This work was supported by the Ministry of Science and Technology of Taiwan R.O.C. under grant NSC101-2221-E-167-020-MY2.

Guo-Shing Huang, is with Department of Electronic Engineering, National Chin-Yi University of Technology Taichung 41101, Taiwan. (corresponding author phone: 886-4-23924505-7338 fax: 886-4-23926610 e-mail: hgs@ncut.edu.tw).

Shing-Lih Wu, is with Department of Mobile Technology, TOKO University, Chiayi 61363, Taiwan. (e-mail: 102020@mail.toko.edu.tw).

Zi-Sheng Lin, is with Department of Electronic Engineering, National Chin-Yi University of Technology Taichung 41101, Taiwan. (e-mail: dan78409@hotmail.com).

II. System Architecture

Figure 1 shows the flow chart of system architecture. Signal productions provide half-bridge circuits by changing signals. And it applies that half-bridge circuits integrate with circuits. It upgrades and outputs current values eventually.

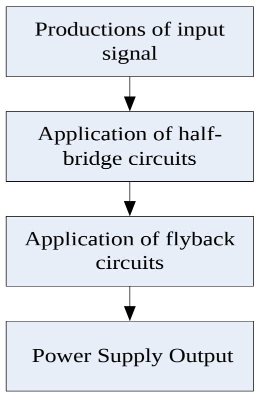

Figure 1 Flowchart of the experiment

A. *Input signal productions*

It controls signals by changing digital signals to produce pulse width modulation, and digital signals are produced from single chip. It adds single chip voltage source to be as voltage regulators to provide required voltage for single chip. Its action principles are as following explanations. It connects pin-18 and pin-19

ISBN: 978-988-19252-7-5
ISSN: 2078-0958 (Print); ISSN: 2078-0966 (Online)

single chip with quartz oscillators and associated circuitry to produce oscillation signals. It operates in coordination with written-inside C language program to control and apply. Hence, it generates the required pulse width modulation signals for front-end converters. It is the signal circuits for digital-signal pulse width modulation as shown in Figure 2 [10].

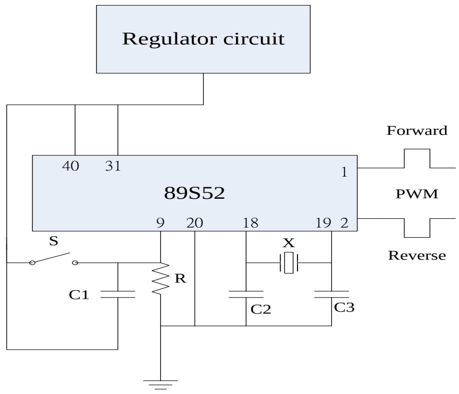

Figure 2 Signal circuit of the PWM

Signals generated from digital signals combine transistor switches to change signals, and it provides the required input signals for front-end half-bridge circuits. As shown in Figure 3 they're signal change circuits. Its action principles are as following explanations. For instance, if input 5 V on-signals, transistor switching output signals are 0 V; if input 5 V off-signals, transistor switching output signals are 18 V and it results in 0-18V and 18-0V pulse width modulation. The thesis applies half-bridge circuits. In terms of signals, we adopt two input signals, and add transistor switches to two input signal backend simultaneously to enhance signals. In addition, it does reverse treatments on signal sources for half-bridge circuits.

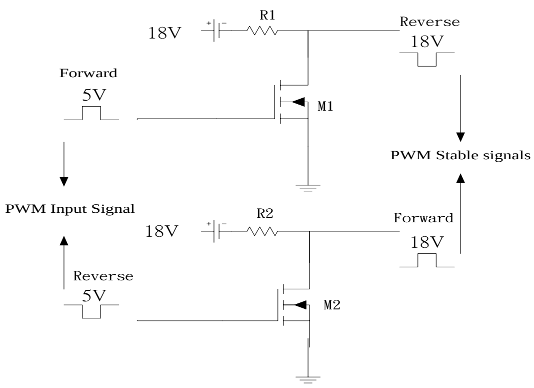

Figure 3 Circuit of the signal change

B. *Application of half-bridge circuits*

Owing to the electric currents and voltages which are square wave, they overlap under conduction and cut and it brings about conversion losses. Moreover, stored capacitance values and inductance values also result in extreme losses from impulse voltages and impulse currents for converters. The conversion losses and conversion impulses are barriers of high frequency, so the upper limit switching frequency of converters is 3 MHz. The experimental frequency is under 20 kHz. Our study takes half-bridge flyback circuits for example, and it upgrades endured load output power values between 10 W and 1 kW. As shown in Figure 4, there are half-bridge circuits in study. Input signals need two signals, one being conducting, and another being non-conducting. In this way, two signals can correspond reversely. With pulse width signals to control conduction band width to generate required duty cycles, it makes more stable pulse voltages for inductor front.

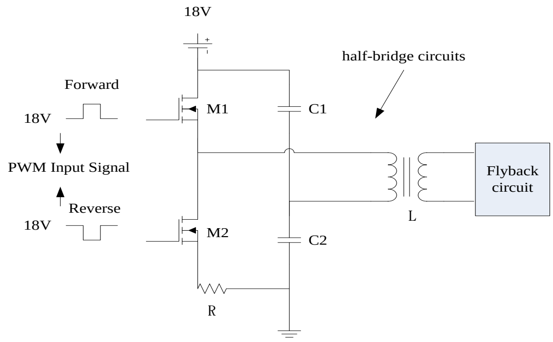

Figure 4 Circuit of the half-bridge

The half-bridge circuit conduction is as shown in Figure 5(a) and (b). Its action principles are as following explanations. For instance, if transistor switches are on, they're conducting; if transistor switches are off, they're non-conducting. To avoid two transistors being conducting at the same time, signals with pulse width signals to control two transistor switches are reverse. As shown in Figure 5(a), it's the circulating mode of M1 transistors conducting. As shown in Figure 5(b), which is the circulating mode of M2 transistors conducting. They are also marked with red arrows.

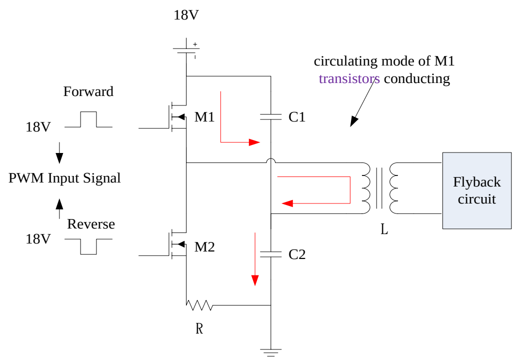

(a) Conducting mode of the M1 transistor

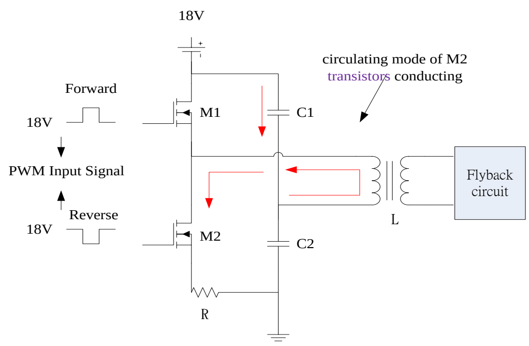

(b) Conducting mode of the M2 transistor

Figure 5 Conducting mode of the half-bridge flyback transistors

ISBN: 978-988-19252-7-5
ISSN: 2078-0958 (Print); ISSN: 2078-0966 (Online)

C. Flyback circuits

Flyback circuits are one kind of buck-boost circuits. They segregate with high-frequency transformers, making input and output not common ground, providing single or multiple fixed output voltages. By closed loop controls, it maintains fixed output voltages when input voltages vary within standard and loads change. As shown in Figure 6 they're flyback circuits [12]. Inductors are divided into two groups of coil winding with boost and buck function. Because inductors affect circuit wastage, converters efficacy have a lot to do with circuit inductors [13]. The paper mainly studies flyback buck circuits generate different efficacy under different frequencies and inductance values. In addition, compare its signal interference to achieve the best conversion efficiency [14-15].

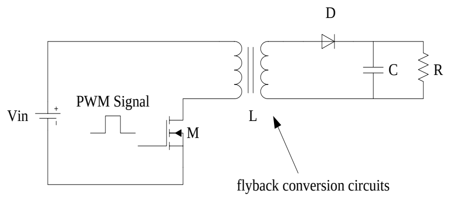

Figure 6 Circuit of the flyback conversion

When switches turn on, it stores energy in input side of inductor primary ring; hence, filter capacitors provide load electric power. When switches turn off, energy stored in inductor primary ring electrify from secondary coils flowing to filter capacitors, and placed at load side simultaneously. There are tremendous rectangular wave currents flowing on filter capacitors, resulting in increased power losses, capacitor temperature rise, and shortening of capacitor life. Moreover, output voltage ripples also increase. For this reason, the study aims at half-bridge flyback circuits. there are flyback circuit conversion action waveforms in Figure 7.

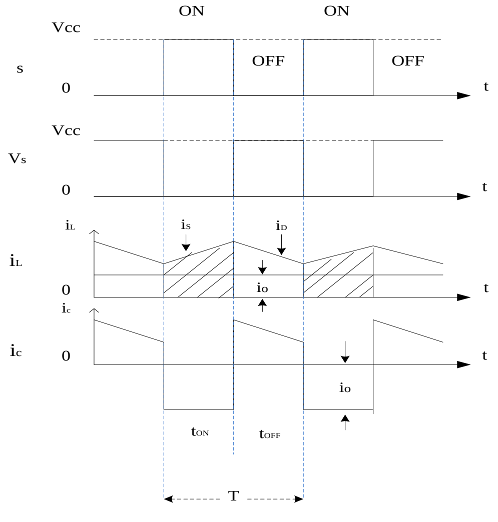

Figure 7 Active waveform of the flyback conversion

Action principles of flyback circuit conversion action waveforms are as following explanations. When switching transistors are t_{ON}, transformer primary N_P is I_P current, and stored energy in that ($E = L_P I_P / 2$). Due to the opposite polarity of N_P and N_S, diodes D are reverse bias and cutoff, no energy delivering to load. When switching transistors are off, according to Lenz's Law, $(e = -N\Delta\Phi / \Delta T)$, transformer primary windings produce an opposite potential, now diodes D are forward direction conducting, IL current flowing to load.

Flyback converters operate in two ways generally:

1. Discontinuous Inductor Current Mode (DCM) or called as "complete energy conversion": All energy stored in transformers at t_{ON} transfers to output side when Timer off in flyback period.
2. Continuous Inductor Current Mode or called as "incomplete energy conversion": A part of energy stored in transformers in the end period of Timer off reserve to the start period of t_{ON}. [16]

III. SYSTEM DESIGN

A. Frequency design

In the pulse width control, it generates signals by Timer0 in Single-chip program. Resolution and frequency of Timer play a vital role in pulse width signals. Take following formula to explain about it [10]:

$$F = \frac{(Focs/12)}{t} \tag{1}$$

F：frequency

t = number of Timer

$Focs$ = Quartz crystal frequency (11.0592MHz and 30MHz)

In a 8bit Timer, Table I shows the when quartz crystal frequency($Focs$) is 11.0592MHz, translation of results of frequency (F) is 3.6KHz, and when quartz crystal frequency($Focs$) is 30.000MHz translation of results of frequency (F) is 9.8KHz, available resolution(t) is 256msec.

Table I The quartz crystal frequency, translation of results of frequency and available resolution

Focs	*t*	*F*
11.0592MHz	256msec	3.6KHz

B. Design duty cycle

With pulse width modulation signals to control duty cycle, it can control overall duty cycle by on-circuits and off-circuits, and with pulse width to control output voltages. Duty Cycle is as following formulas [10]:

$$\text{Duty Cycle} = \frac{t_H}{t_H + t_L}\% \tag{2}$$

Duty Cycle：duty cycle

t_H ：time of high electric potential

t_L ：time of low electric potential

Assume that input signal voltage value is 18V and output signal voltage value is 12V, it can calculate that t_H is about 66.6% and t_L is about 33.3%. Duty Cycle can be computed from input and output circuit voltage values list in Table II.

ISBN: 978-988-19252-7-5
ISSN: 2078-0958 (Print); ISSN: 2078-0966 (Online)

Table II The duty cycle, input circuit voltage and output circuit voltage

V_{in}	V_{out}	Duty Cycle	t_H	t_L
18V	12V	0.66%	0.66%	0.33%

C. *Inductor Design*

Inductors are important part in flyback circuits. Different frequencies and inductance values affect transformation efficacy, and high- frequency inductor design needs many steps to proceed. The followings can be divided into several items to design it, and therefore achieving the required inductance values for the experiment. As shown in Figure 8, it's the basic flowchart for design inductance values [9].

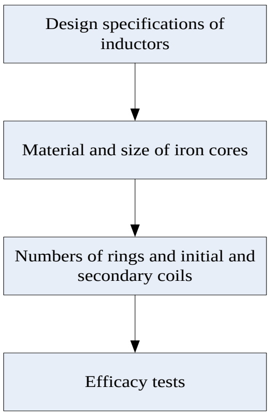

Figure 8 Design steps of the inductors

(a) Specifications of inductors

Set input and output voltages and currents, output wattages, coil thickness and switching frequency, and so on. The computations of primary inductor current and inductance values are as followings.

$$I_{pp} = \frac{2 * P_o}{V_{in(\min)} * Duty} \quad (3)$$

$$L_P = \frac{V_{in(\min)*} Duty}{I_{pp} * f} \quad (4)$$

I_{PP} ：primary current values

P_o ： output electric power

$V_{in(\min)*}$ ：input voltages(minimum value)

$Duty$ ：duty cycle

L_P ：primary inductance values

f ：frequency

(b) Material and size of iron cores

The market is almost full of high-frequency inductor iron cores made by ceramic magnets. Its advantages are low costs, high reluctances, frequency range (5 kHz ~200 kHz) and high stability.

Following formula can determine the size of iron cores:

$$\mathrm{AP} = \frac{P_{out} * D}{K * \eta * \Delta\mathrm{B} * J * f} * 10^8 \quad (5)$$

AP：size of iron cores

P_{out} ：output wattages

D：duty cycle

K ：coiling factors(for example, K value of type E, U and I is 0.6)

η ：efficiency

$\Delta\mathrm{B}$ ：Operating flux density

J：Current Density

f：Operating Frequency

(c) Initial and secondary coils

Coils are determined by main N_P, and initial coils to secondary coils ratio is $\frac{N_P}{N_S} = \frac{V_P}{V_S}$.

$$N_P(\min) = \frac{V_{in} * \Delta t}{A_e * \Delta B} \quad (6)$$

V_{in} ：input voltage

Δt duty cycle

A_e ：grille square measure of iron cores

With above formulas, it can compute inductance values of inductors. Table III shows assume that P_o is 36W, $V_{in(\min)*}$ is 18V, $Duty$ is 0.66, f is 10 KHz, to compute inductance values, current value I_{pp} is 6A. Then calculate the inductance values L_p is 200 μ H.

Table III The inductance values and current value

P_o	$V_{in(\min)*}$	$Duty$	f	I_{pp}	L_P
36W	18V	0.66	10 KHz	6A	200 μ H

IV. Experimental Test Results

A. *Experimental signal generation*

It is the experimental waveform diagram of input signal generation as shown in Figure 9, and it makes double-waveform reverse. The digital signal voltage is 5V generating from embedded single chip.

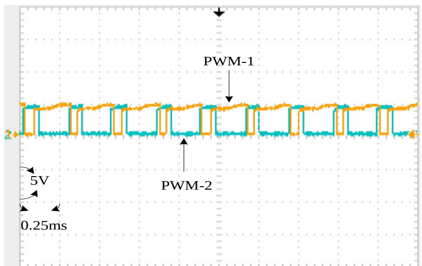

Figure 9 The voltage waveform diagram of the voltage 5V

In Figure 10, it is the waveform diagram of voltage 18V through transistor switch changing to let waveform be shown in Figure 10, it can execute the half-bridge circuit application. It should set front-end digital signals, so reverse waveform can operate.

ISBN: 978-988-19252-7-5
ISSN: 2078-0958 (Print); ISSN: 2078-0966 (Online)

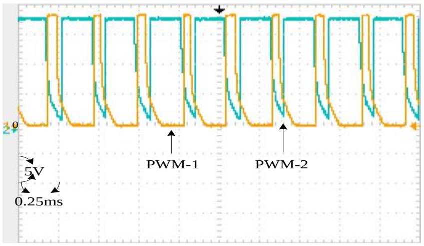

Figure 10 The voltage waveform diagram of the voltage 18V

B. *Output Current Test*

As shown in Figure 11, it conducts current tests on output voltage 12V to purely resistive of load 10 ohms. Through the rising current circuit to improve the stability and reliability of current, it can supply output current continuously.

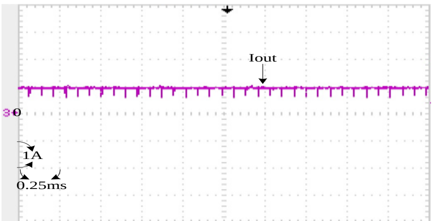

Figure 11 The test currents of the purely resistive load

C. *Test signal interference with different frequencies and inductance values*

The following waveform diagram is measured with 3.6 kHz frequencies. As shown in Figure 12, it is L_P and L_S waveform diagram of 1：1 inductors (inductance value is 9.68mH) bought from the markets. Waveforms are electric currents on converters flowing through inductors to generate changing voltage waveform diagram.

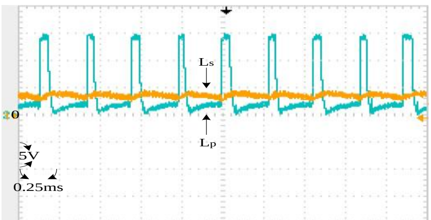

Figure 12 The voltage waveform diagram of the commercial inductors L_P and L_S

As shown in Figure 13, there are the waveform diagram of inductors L_{P1} front-to-ground and the waveform diagram of inductors L_{P2} end-to-ground.

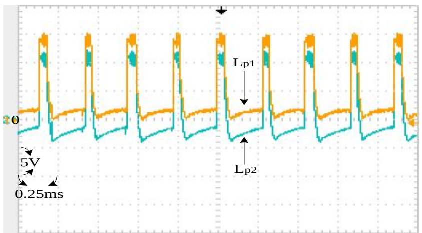

Figure 13 The voltage waveform diagram of the commercial inductors L_{P1} front-to-ground and L_{P2} end-to-ground

As shown in Figure 14, it is L_P and L_S waveform diagram of 1：1 inductors (inductance value is 200 μH) self-winding. Waveforms are electric current on converters flowing through inductors to generate changing voltage waveform diagram.

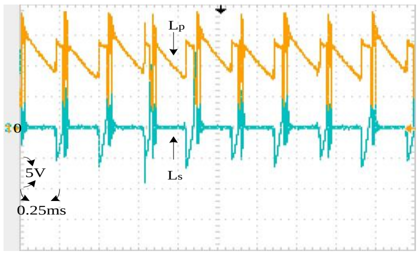

Figure 14 The voltage waveform diagram of the self-winding inductors L_P and L_S

As shown in Figure 15, there are the waveform diagram of inductor L_{P1} front-to-ground and the waveform diagram of inductor L_{P2} end-to-ground.

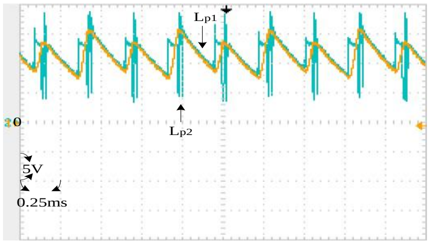

Figure 15 The voltage waveform diagram of the self-winding inductors L_{P1} front-to-ground and L_{P2} end-to-ground

The following waveform diagram is measured with 9.8k Hz frequencies. As shown in Figure 16, it is L_P and L_S waveform diagram of 1：1 inductors (inductance value is 9.68 mH) bought from the markets. Waveforms are electric currents on converters flowing through inductors to generate changing voltage waveform diagram.

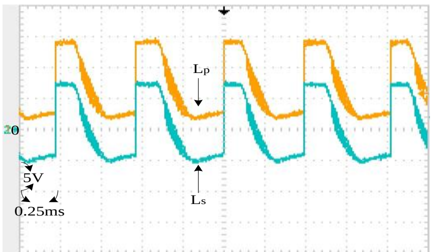

Figure 16 The voltage waveform diagram of the commercial inductors L_P and L_S

As shown in Figure 17, there are the waveform diagram of inductor L_{P1} front-to-ground and the waveform diagram of inductor L_{P2} end-to-ground.

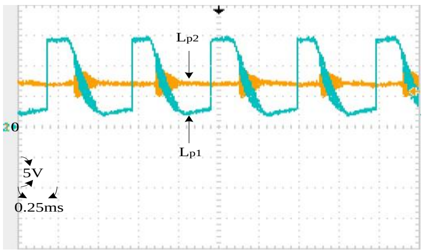

Figure 17 The voltage waveform diagram of the commercial inductors L_P front-to-ground and end-to-ground

ISBN: 978-988-19252-7-5
ISSN: 2078-0958 (Print); ISSN: 2078-0966 (Online)

As shown in Figure 18, it is L_P and L_S waveform diagram of 1：1 inductors (inductance value is 200 μ H) self-winding. Waveforms are electric currents on converters flowing through inductors to generate changes as voltage waveform diagram.

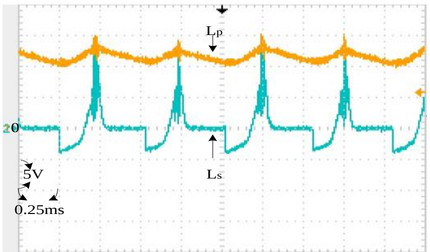

Figure 18 The voltage waveform diagram of the self-winding inductors L_P and L_S

As shown in Figure 19, there are the waveform diagram of inductor L_{P1} front-to-ground and the waveform diagram of inductor L_{P2} end-to-ground.

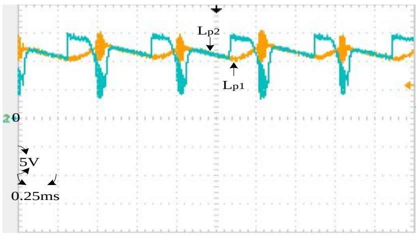

Figure 19 The voltage waveform diagram of the self-winding inductors L_P front-to-ground and L_S end-to-ground

As shown in Table IV, which is the L_P and L_S comparison of interference noise and steady state waveform. According to waveform diagrams tested from above experiments, it completes the comparison table.

Table IV The L_P and L_S comparison of interference noise and steady waveform

F	L	L_P 、L_S Clutter signal interference	L_P 、L_S Steady state waveform
3.6kHz	9.68mH	Relatively poor	Relatively poor
3.6kHz	9.67mH	Relatively poor	Relatively poor
3.6kHz	200 μ H	Relatively poor	Relatively better
3.6kHz	200 μ H	Relatively poor	Relatively better
9.8kHz	9.68mH	Relatively better	Relatively poor
9.8kHz	9.68mH	Relatively better	Relatively poor
9.8kHz	200 μ H	Relatively better	Relatively better
9.8kHz	200 μ H	Relatively better	Relatively better

Experimental measurements compare commercial inductors with self-winding inductors, with 3.6 kHz to 9.8kHz frequencies. Frequencies affect the shock waveform. According to experimental measurements, the best waveform is 9.8 kHz frequencies with self-winding inductors.

V. CONCLUSION

In terms of hardware circuits, we use pulse width signals, half-bridge circuit, flyback, rising current circuit and with self-winding inductor to combine the best converter; flyback circuits combined with half-bridge circuits can greatly enhance the load electric power, so the maximum power value of load output can bear about 1kW. Rising current circuit makes the output current circuit more stable, and then completes the half-bridge flyback converter. According to the experimental data, it can be learned about the dependencies and importance between frequencies and inductance values. When the frequency is 9.8 kHz and inductance value is 200 μ H, the output voltage waveform is the best one. Advantages of the converter are higher output power, high operating efficiency, small size circuits, tractable signals and low cost.

References

[1] J. Sha, J. Xu, B. Bao, and T. Yan, "Effects of circuit parameters on dynamics of current mode pulse train contro lled buck converter," *IEEE Transactions on Industrial Electronics*, vol.61, pp. 1562 – 1573, June 2014.

[2] S.-K. Kim, C. R. Park, J.-S. Kim, and Y. I. Lee, "A stabilizing model predictive controller for voltage regulation of a DC/DC boost converter," *IEEE Transactions on Control Systems Technology*, 2014.

[3] M. Pavlovsky, G Guidi, and A. Kawamura, "Buck/boost DC–DC converter topology with soft switching in the whole operating region," *IEEE Transactions on Power Electronics*, vol. 29, pp.851 – 862, June 2014.

[4] J. -Y. Chen, and Z. -X. Lin, "LFR dynamic analysis and design of a novel single-stage diagonal half-bridge flyback converter with power factor correction," National Cheng Kung University Department of Engineering Science Master Thesis, 2006.

[5] S. -C. Tong, and S. -L. Huang, "The study of bidirectional DC-DC converter for DC system", Feng Chia University Department of Electrical Engineering Master Thesis, 2010.

[6] D. Murthy-Bellur, and M. K. Kazimierczuk, "Zero-current-transition two-switch fyback pulse-width modulated DC –DC converter," *IET on Power Electronics*, vol. 4, pp. 288 – 295, June 2011.

[7] Z. -S. Ling, T. -J. Liang, L. -S. Yang and T. -H. Li, "Design and implementation of quasi-resonant DC-DC flyback converter," *International Conference on Power Electronics and Drive Systems*, pp. 429 – 433, PEDS 2009.

[8] F. Zhang, L. Xiao, and Y. Yan, "Bi-directional forward-flyback DC-DC converter," *IEEE 35th Annual on Power Electronics Specialists Conference*, pp. 4058 – 4061, 2004.

[9] R. -J. Hu, and C. -L. Chen, "On-line DSP-based uninterruptible power supply," NSYSU Department of Electrical Engineering Master Thesis, 2001.

[10] X. -S. Chen, and G. -S. Huang, "Development of dual robotic arm system based on binocular vision," *CACS* 2013.

[11] K. Harada, "Switching power technical manual," Jian hsin Publishers.

[12] E. V. D. Souza, and I. Barbi, "Bidirectional current-fed flyback-push-pull DC-DC converter," *Power Electronics Conference* (*COBEP*), pp. 8 - 13, 2011.

[13] H. Eyhani, and H. Toliyat, "Partial-resonant buck-boost and flyback DC-DC converters," *IEEE Transactions on power Electronics*, 2014.

[14] A. Emrani, E. Adib, and H. Farzanehfard, "Single-switch soft-switched isolated DC–DC converter," *IEEE Transactions on Power Electronics*, vol. 27, pp. 1952 – 1957, June 2012.

[15] H. Keyhani, and H. Toliyat, "Partial-resonant buck-boost and flyback DC-DC converters," *IEEE Transactions on Power Electronics*, 2014.

[16] S. W. Lee, K. -S. Choi, B. -H. Cho and B. C. Hyun, "A center-tapped forward-flyback DC/DC converterfor low power application", *Energy Conversion Congress and Exposition* (*ECCE*), 2013.

ISBN: 978-988-19252-7-5
ISSN: 2078-0958 (Print); ISSN: 2078-0966 (Online)